Smart charging of electric bus fleet minimizing battery degradation at extreme temperature conditions

Adnane Houbbadi, Eduardo Redondo-Iglesias, Serge Pelissier, Rochdi Trigui, Tanguy Bouton

Smart charging of electric bus fleet minimizing battery degradation at extreme temperature conditions

Adnane Houbbadi[2], Eduardo Redondo-Iglesias[1*], Serge Pelissier[1], Rochdi Trigui[1] and Tanguy Bouton[2]
[1]*AME-Eco7, Univ Gustave Eiffel, Bron, France*,
[2]*TRANSDEV GROUP, Issy-les-Moulineaux, France*
[*]corresponding author: eduardo.redondo@univ-eiffel.fr

***Abstract*—This paper presents an optimized control strategy for lithium-ion batteries lifetime used on electric buses at high and low temperatures. In high temperature environments, the main aging mechanism is the formation and growth of the solid electrolyte interface. This mechanism is typically related to calendar aging and amplified at higher state of charge and temperature. On the other hand, at low temperature, the deposition of lithium metal (lithium plating) is predominant only during cycling and battery degradation increases as the temperature drops. All these factors could greatly increase the battery degradation. A novel battery aging model based on Eyring's laws is developed considering different aging mechanisms particularly subject to extreme temperature conditions at rest and charging scenarios. Based on this model, the aging is quantified and optimized through an optimization methodology under several scenarios. The simulation results show that the charging strategy becomes necessary at extreme temperature conditions and is able to save on vehicle operation costs.**

***Index Terms*—battery aging, electric buses, optimization, smart charging**

I. Introduction

Electro-mobility is increasing significantly in the urban public transport. However, a massive deployment of electric buses (EBs) could overload the power grid and produce network congestion problems generating power peaks [1]. On the other hand, the EBs purchase costs should be mitigated by low operational costs.

To this end, many fleet operators seek to optimize the operation cost of EB. The electric vehicles (EVs) smart charging is one of the main tools to be deployed. Several optimization methods had been used to optimize large and small-scale EVs fleets through an extensive literature review [2]. Other works [3]–[12] have investigated overnight charging on centralized bus depots of an EBs fleets. They analyzed large and small-scale bus depots to minimize the operational costs or the load peak or the calendar aging of the batteries.

In this work, we will present a new approach for optimization of lithium-ion batteries lifetime used on EBs at high and low temperatures.This approach combines an electro-thermal aging behavior and uses a nonlinear programming (NLP) algorithm. A novel battery aging model that separates cold and hot temperature aging mechanisms and combines calendar and cycling aging has been developed.

The remainder of the paper is structured as follows. In Section II, a new approach for smart charging strategy of EBs is introduced with the system modeling. In this section, a dynamic battery aging model is developed. This model takes into account different aging mechanisms particularly subject to extreme temperature conditions at rest and charging scenarios. Section III presents the mathematical formulation of the mono-objective optimization problem of EBs fleet charging. In Section IV a case study of an EB operating in a depot is presented. The results of optimal charging following two different scenarios are included in Section V. Finally, we draw some conclusions and introduce future work.

II. System modeling

The modeling of the battery consists of an electro-thermal model coupled to an aging model. A converter model is integrated in order to take into account the efficiency of AC/DC and DC/DC conversions.

A. Electro-thermal battery model

We used an equivalent electrical circuit developed on VEHLIB for the electrical model [13]. The thermal model used a prismatic lithium-ion battery model (LiFePO4/graphite) based on an equivalent electrical circuit. The equivalent electric circuit equation is presented below :

$$U_{bat} = OCV - R_{eq} * I_{bat} \tag{1}$$

Where I_{bat} is the battery charge current, U_{bat} is the battery voltage, OCV is the open circuit voltage, R_{eq} is the internal resistance of the battery. The electro-thermal coupling equation is presented below :

$$C_{th}\frac{dT_{bat}}{dt} = I_{bat}\left(U_{bat} - OCV\right) - h\left(T_{bat} - T_{amb}\right) \tag{2}$$

Where T_{bat} is the battery temperature, T_{amb} is the ambient temperature, h is the heat transfer coefficient, OCV is the open circuit voltage, C_{th} is the specific thermal capacity of the battery.

In our previous work [14], we estimated the heat capacity and heat transfer coefficient by performing some experiments. These results were compared with experimental values from

the literature. The battery pack configuration will strongly impact on the battery thermal characteristics. For this reason, we assumed that we have a configuration with no thermal insulation, homogeneous temperature in the battery pack, no cooling system and no forced air convection similar to that of [14]. The battery pack electro-thermal parameters are presented in Section IV, Table II.

B. Converter model

A simple converter model has been developed to represent the charger efficiency. Electrical power is converted from the grid to the battery through an AC/DC and DC/DC converter. Experimental results of charger efficiency have been used as a converter model to stay in an acceptable simulation time [15]. In a first approach, we used a linear interpolation of charger efficiency values until we develop a specific converter model. These values are based on the experimental results mentioned above.

C. Dynamic battery aging model

Battery characteristics degrade over time due to aging mechanism. Each aging mechanism can be seen as a physicochemical reaction (or a combination of several reactions). Those mechanisms produce a loss of capacity and/or an impedance rise and they depend mainly on three factors: temperature, state of charge (SoC) and current.

Typically, battery aging is classified in calendar aging ($I = 0$) or cycling aging ($I \neq 0$). For lithium-ion batteries, the main calendar aging mechanism is formation and growth of the solid electrolyte interface (SEI) layer on the negative (graphite) electrode. The main factors accelerating this mechanism are temperature and SoC. At higher temperatures and SoC levels, SEI formation is accelerated. This aging was modelled with a modified Arrhenius law [16]–[18] or more recently with Eyring law [19]. When lithium-ion batteries are cycled at cold temperatures, another aging mechanism may degrade them: the lithium plating of the negative electrode. This mechanism is amplified with colder temperatures and higher SoC levels (battery charge).

As shown in Fig.1, battery degradation rate at hot temperatures can be fitted to an Arrhenius plot (blue points), where the slope is the activation energy of the reaction. At cold temperatures, the battery degradation rate trend is inverted and in this case, a negative slope is found in the Arrhenius plot.

Song et al. [21] modelled LFP battery aging in cycling at a broad range of temperatures with an empirical model based on a modified Arrhenius law. The absolute value function has been introduced by Song in equation (3) in order to take into account the reversal of the aging trend with the temperature below a certain value:

$$\frac{dQ_L}{dAh} = A \cdot exp\left(\frac{-E_a + C \cdot I}{z \cdot R \cdot (|285.75 - T| + 265)}\right) \cdot Q_L^{\frac{z-1}{z}} \quad (3)$$

where A and C are constants, R is the universal gas constant, z is an exponent between 0 and 1, E_a is an activation energy,

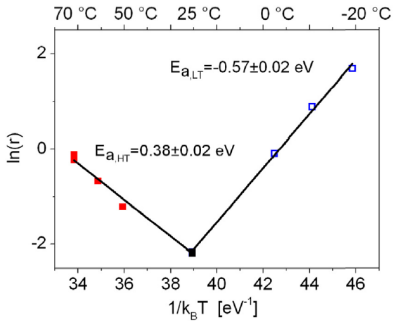

Fig. 1. Arrhenius law for the aging of 18650 cells cycled at 1 C in a temperature range between -20 and +70 C [20]

I is the current, T is the temperature and Q_L is the capacity loss. However, model expressed by equation (3) does not fulfill several requirements to our application:

i the use of the absolute value in the modified Arrhenius law.

ii this model is expressed in equivalent full cycles (from SoC100 to SoC0 and to SoC100 again) and considering the same current rate at charge and at discharge.

The first consequence for (i) is that the absolute value function could bring numerical issues in the optimization problem process. Moreover, the absolute value implies that model behavior is symmetrical with temperature (same slope but negative value at cold temperatures) but it could not be the case for every battery technology. For example, in Fig. 1, the slopes are respectively 0.38 and -0.57eV.

The consequence of (ii) is that with this type of model, it is not possible to consider complex cycling profiles, for example, in our application a variable power charge profile.

Finally, SoC influence on cycling or during rest periods is not considered in this type of model, while it could have an important role in battery degradation in slow charge.

In this work, we propose to use a multi-mechanism model based on Eyring laws in which the capacity loss rate dQ_L/dt is divided in contribution of calendar, cycling at hot temperature and cycling at cold temperature:

$$\frac{dQ_L}{dt} = \frac{dQ_{L,cal}}{dt} + \frac{dQ_{L,cyc,hot}}{dt} + \frac{dQ_{L,cyc,cold}}{dt} \quad (4)$$

with:

$$\frac{dQ_{L,cal}}{dt} = A_{cal} \cdot e^{\left(\frac{-E_{a,cal}}{kT} + B_{cal} \cdot SoC\right)} \cdot f(Q_L) \quad (5)$$

$$\frac{dQ_{L,cyc,hot}}{dt} = A_h \cdot e^{\left(\frac{-E_{a,h} + C_h \cdot I}{kT} + B_h \cdot SoC\right)} \cdot f(Q_L) \quad (6)$$

$$\frac{dQ_{L,cyc,cold}}{dt} = A_c \cdot e^{\left(\frac{-E_{a,c} + C_c \cdot I}{k(T_r - T)} + B_c \cdot SoC\right)} \cdot f(Q_L) \quad (7)$$

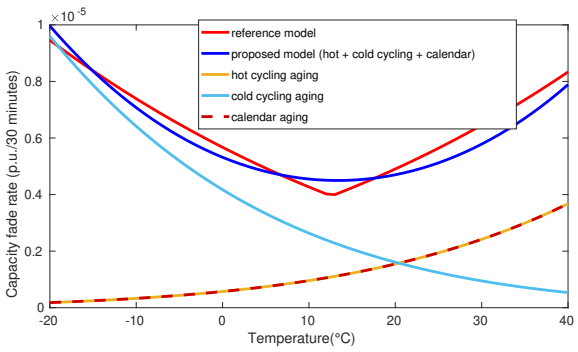

Fig. 2. Capacity fade of 30 minutes of charge at C/6, initial SoC = 50% and initial capacity fade = 1%

$$f(Q_L) = \left(\frac{1}{1 + b \cdot Q_L^c}\right) \tag{8}$$

In each Eyring law (eqs. 5 to 7) A_i is the pre-exponential term, $E_{a,i}$ is the activation energy, B_i is the SoC influence parameter and C_i is the current influence parameter (with index $i = cal, h, c$ for calendar, hot cycling and cold cycling respectively). k is the Boltzmann constant, T is the battery temperature, I is the current and SoC is the state of charge. Eq. 7 is an Eyring type formulation modified to inverse the temperature effect. Eq. 8 represents the dependence of Q_L in $\frac{dQ_L}{dt}$. For example, SEI growth leads to a diminution of $\frac{dQ_L}{dt}$ as found in [22]. For simplicity reasons, in this work the same parameters of $\frac{dQ_L}{dt}$ decay (b, c in eq. 8) are chosen for calendar, hot cycling and cold cycling.

Model described by equations 4 to 7 has been calibrated to fit model of equation 3 in a large range of temperatures (from -20 to 40°C) and Q_L (from 0 to 0.3 p.u.). To introduce the SoC influence on aging the parameter B was fixed to the same value obtained in [19] (B=1.104 p.u.), for calendar (B_{cal}), hot (B_h) and cold (B_c) cycling laws. The values of all identified parameters are shown in table II.

Figure 2 illustrates the temperature dependence of the reference model (equation 3) compared with that of the proposed model (equation 4). This figure also shows the decomposition of capacity fade made with each component of capacity fade: calendar, hot cycling and cold cycling (respectively equations. 5, 6 and 7).

III. Mono-objective optimization methodology for EBs fleet charging

The methodological approach has been developed in Matlab environment to optimize an EBs fleet overnight charging. The aim is to optimize the charging power profile in order to minimize a fitness function while respecting all the constraints. The algorithm used to solve the optimization problem is the nonlinear programming (NLP). The fitness function is evaluated using a converter and a battery model. The optimization takes into account different constraints:

- Operating constraints (number of buses, arrival and departure time...)
- Battery and environmental constraints (battery temperature (T), ambient temperature, initial state of charge (SoC) and the targeted SoC)
- Charging infrastructure constraints (maximum charging power, number of charging points, ...)
- Power grid constraints (power peak demand...)

In this work, the optimization variable is the charging power P of the bus fleet represented in an $(n \times m)$ matrix:

A. Optimization variable

$$P = \begin{pmatrix} p_{1,1} & \cdots & p_{1,m} \\ \vdots & \ddots & \vdots \\ p_{n,1} & \cdots & p_{n,m} \end{pmatrix} = (p_{i,j}); \begin{cases} i = 1 \ldots n \\ j = 1 \ldots m \end{cases} \tag{9}$$

Where i is the number of EBs and j represents the time slots, $p_{i,j}$ is the charging power for EB number i during a time slot j .

B. Objective function

The goal is to minimize the battery aging. The battery aging can be formulated in the equation bellow:

$$objective = min \sum_{i=1}^{n} \sum_{j=1}^{m} \frac{dQ_{L_{i,j}}}{dt} \tag{10}$$

The battery aging represents the capacity loss of the battery. $\frac{dQ_{L_{i,j}}}{dt}$ is the capacity loss rate of EB number i during a time slot j (p.u./day).

C. Linear equality and inequality constraints

First constraint is the maximum charging power of each charging point, all elements of the optimization variable $p_{i,j}$ have to respect the maximum charging power p_{max}:

$$0 \leq p_{i,j} \leq p_{max} \tag{11}$$

The second constraint is the total subscribed power for the charging station, that is the maximum simultaneous demanded power to the electricity provider: each column vector $P_{\{j\}}$ $(n \times 1)$ of the matrix P has to respect the charging infrastructure subscribed power $p_{subscribed}$, A_s is an all-ones $(1 \times n)$ matrix:

$$A_s \times P_{\{j\}} \leq p_{subscribed} \tag{12}$$

The equation above means that the sum of all charging points at each moment must be lower or equal to $p_{subscribed}$.

$$A_e \times P_{\{i\}}^T = 0 \tag{13}$$

The transpose $P_{\{i\}}^T$ $(m \times 1)$ of the row matrix $P_{\{i\}}$ must respect the bus departure and arrival times, A_e is a column matrix $(1 \times m)$ with all-ones when the bus is out of the depot, otherwise A_e takes the value 0 between the bus arrival and departure time.

$$A_n \times P_{\{i\}}^T = \frac{(SoC_{final} - SoC_{initial}) \times C_{bat} \times \overline{OCV_{bat}} \times 100}{\Delta t \times \overline{\eta_{ch}} \times \overline{\eta_{bat}}} \quad (14)$$

The transpose $P_{\{i\}}^T$ of the row matrix $P_{\{i\}}$ has to respect the amount of energy required to reach the targeted SoC_{final}. A_n is an all-ones row matrix, Δt the time-slot of 30 min (h), C_{bat} is the total battery capacity (Ah), $\overline{OCV_{bat}}$ the average battery open-circuit voltage (V), $\overline{\eta_{ch}}$ is the average charger efficiency (%) and $\overline{\eta_{bat}}$ is the average battery efficiency (%). The average values are estimated during a pre-optimization process as explained in [14].

IV. Case Study

To illustrate the optimization of an EBs fleet, a case study was performed. Our optimization tools are able to manage fleets composed of several EBs [23]. However, for simplicity reasons, in this example a fleet composed of only one EB is considered. When several EBs are considered, different conditions can be considered for each EB (temperature, initial and final state of charge, etc.).

The EB fleet operates an existing conventional bus line during the day. Once the operation is finished, the EB fleet returns to the depot and the optimization takes place. The charging period of 14 hours occurs at the depot (from t_0 to t_0 + 14h) divided into 27 time-slots of 30 min each, which results in a reasonable search space. Table 1 and 2 present the simulation parameters and battery pack electro-thermal and aging characteristics.

TABLE I
Simulation parameters and operating constraints.

Parameter	Value
Number of buses	1
Number of simulated days	1 day
Charging time period	14 hours
Number of charging time slots	27
Time slot	30 minutes
Initial SoC day J	10%
Targeted SoC day J+1	100%
Distance to be covered day J+1	200 km

V. Results

A. Optimization of a daily charging schedule at hot temperature

In the first scenario, we will present some results of the proposed method by minimizing the battery aging of one EB at hot temperature during one night. The initial and ambient simulation conditions are:

- Ambient temperature: 30°C
- Initial battery temperature: 35°C
- Initial battery capacity loss: 0%

The battery aging optimization results at hot temperature in Fig.3 show that the algorithm decides to wait until the battery temperature drops, where the calendar aging is always present and predominant (hot cycling at max current slightly exceeds the calendar only effect), therefore the algorithm will further minimize the calendar. The optimal solution tends to increase the power gradually, this could be explained by the fact that the objective function (9) depends on SoC, battery temperature and the current as well as the effect of their interaction. To minimize battery aging, the optimal charging

TABLE II
Battery electro-thermal aging characteristics.

Parameter	Value
Battery type	LIFePO4
Nominal energy/capacity	311 kWh / 540 Ah
Pack surface for thermal exchange	18.79 m2
Weight	2500 kg
Specific heat capacity	900 J.kg -1 .K -1
Heat transfer coefficient	5 W.m -2 .K -1
A_{cal} : Pre-exponential factor	0.17e+02 p.u.day -1
A_h : Pre-exponential factor	1.06e+02 p.u.day -1
A_c : Pre-exponential factor	2.12e+02 p.u.day -1
$E_{a,c} = E_{a,h}$: Activation energy	0.344eV
$E_{a,cal}$: Activation energy	0.343eV
$C_c = C_h$: Current coefficient	0.019 hour.p.u -1
T_r : Reference temperature	571,5 K
k : Boltzmann constant	8.617×10 -5 eV.K -1
$B_{cal} = B_c = B_h$: charge factor	1.104 p.u -1
I_0 : Current calendar calibration	C/12 p.u.hour -1
b : Coefficient	63
c : Coefficient	0.18

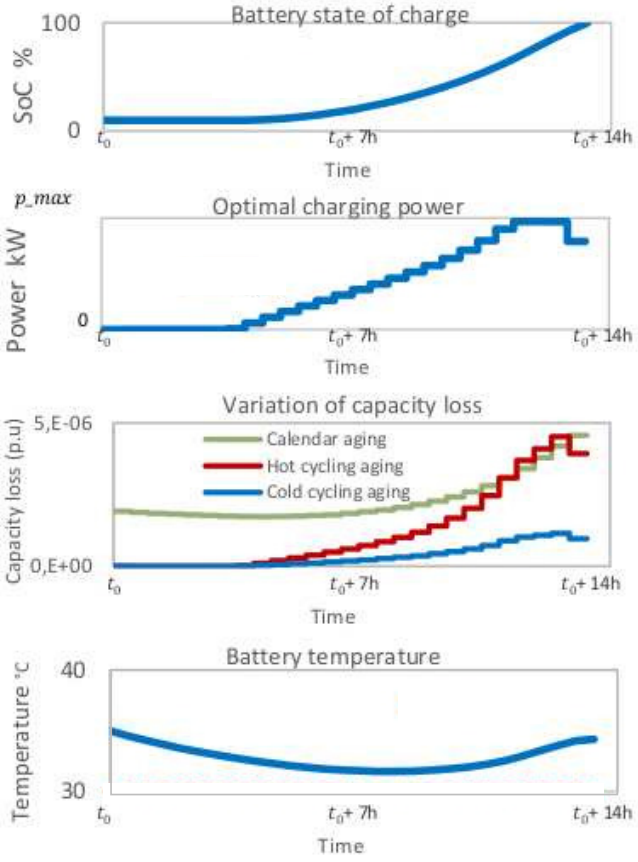

Fig. 3. Optimization to minimize battery aging for one EB at hot temperature (30°C): scenario 1

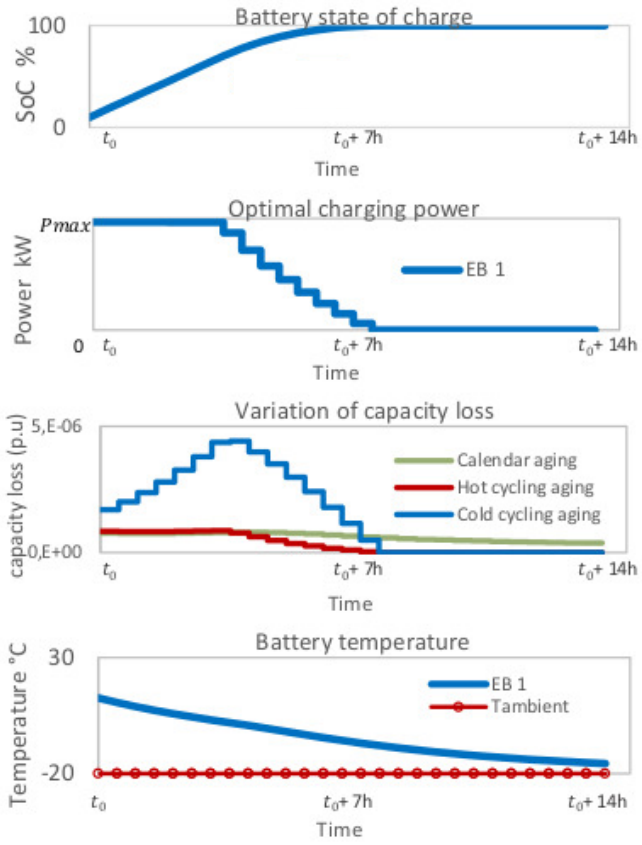

Fig. 4. Optimization to minimize battery aging for one EB at cold temperature (-20°C): scenario 2

power profile delays the charge to reach higher values of SoC as late as possible and increases the power gradually to avoid battery overheating. Calendar aging is always present and preponderant. Cycling will have a great influence for temperatures below 0 ° C. Therefore, we will see how the algorithm performs at extreme temperature conditions.

B. Optimization of a daily charging schedule at cold temperature

In this scenario, we use the same simulation parameters and operating constraints as the first scenario, except the temperature conditions. The initial and ambient simulation conditions are:

- Ambient temperature: -20°C
- Initial battery temperature: 12°C
- Initial battery capacity loss: 0%

The battery aging optimization results at cold temperature in Fig.4 show that the algorithm decides to charge the battery as soon as possible at maximum power in order to keep the battery at positive temperatures. The more the battery temperature drops due to heat losses, the more the algorithm will gradually decrease its power because cold cycling becomes predominant. In this scenario, we can notice that the calendar

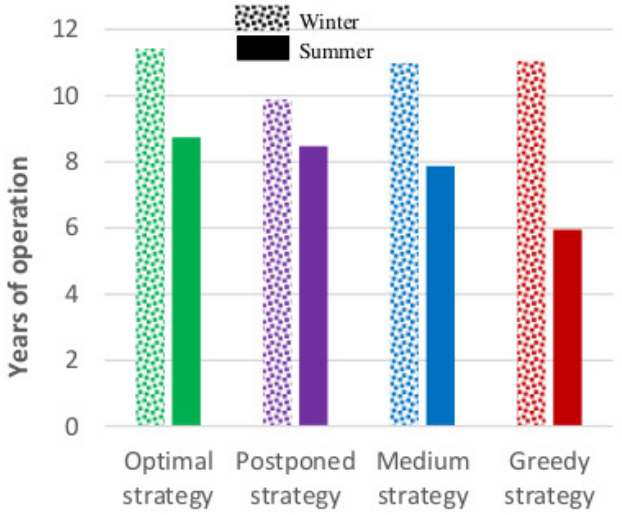

Fig. 5. Operating period at 20% capacity loss, Summer and winter scenario

aging becomes negligible compared to the cycling aging at cold temperature.

C. Optimization of a long operating period at various temperature

To illustrate the potential economic savings, a battery aging optimization of one EB for a long period of operation will be performed. The same operating constraints in the Table 1 have been used. Three typical charging strategies will be used as references:

- The “Greedy” baseline: maximum charging power is used as soon as possible until it is fully charged.
- The “Medium” baseline: an average charging power is used throughout the charging period.
- The “Postponed” baseline: maximum charging power is used as late as possible until it is fully charged.

These strategies represent a daily optimized solutions. These solutions will be projected over a long period of vehicle operation, assuming that the same charging strategies are used every day. The battery aging during bus operation will not be taken into account, only the battery aging at night (from t_0 to t_0+14h) is considered. The simulation of battery aging over a long period was made by simulating the daily optimized strategies and by calculating the daily capacity loss while considering the effects of previous aging. We used the same optimal charging strategy throughout the bus operation, the strategy does not change even if the battery ages.

The simulation was performed considering a succession of identical days (winter or summer). Such a non-realistic scenario intended to view the difference in degradation for the different strategies. The results of the simulation in Fig.5 indicate that the optimal strategy is the most profitable strategy whatever the temperature is. During winter, it is recommended to charge as soon as possible to heat the battery. This relates to the greedy baseline strategy and medium strategy. During

summer, it is recommended to charge progressively as late as possible as the postponed baseline strategy.

Based on our simulation, the optimal strategy uses the battery 30% less compared to greedy strategy in summer. In winter the gain on lifetime is lower. But it must be underlined that the optimal strategy enables to respect the operating constraints of a fleet of buses, contrary to all other strategies. It should be noted that the optimization results strongly depend on the model of electro-thermal aging of the battery in Table 2.

VI. Conclusion and future works

This paper introduces a smart charging methodology to minimize battery aging of EBs. We presented a novel battery aging model based on Eyring's law. This model separates cold and hot temperature aging mechanisms and combines calendar and cycling aging. It has several advantages compared to the reference aging and existing model (3). The first is the continuity and differentiability of the function throughout the area of use. The second is its adaptability: our model can be adapted to different battery technologies according to their sensitivity to low / high temperatures, cold or hot cycling.

A case study is performed using our developed battery aging model to minimize battery degradation. The implemented optimization algorithm is efficient and provides quick search result after only 2 min of computing time for one EB. The algorithm is also able to deal with large fleet of several hundred buses. The simulation results of mono- objective optimization of battery aging show that the optimal strategy charges the EB gradually and reach high SoC values as late as possible for hot temperature conditions. During cold temperature, the simulation results show that the algorithm decides to charge the battery as soon as possible at maximum power in order to keep the battery at positive temperatures. In this scenario, it has been noticed that calendar aging becomes negligible compared to aging during cycling at very low temperatures.

In future work, the idea is to expand the methodology to a larger size of EB fleets. A multi-objective optimization should be performed too. The battery thermal and aging model sensitivity has to be carefully studied as well as the battery pack configuration.

References

[1] M. Dietmannsberger, M. Schumann, M. Meyer, and D. Schulz, in *1st E-Mobility Power System Integration Symposium*, 2017, p. 8.

[2] J. Hu, H. Morais, T. Sousa, and M. Lind, *Renewable and Sustainable Energy Reviews*, vol. 56, pp. 1207–1226, 2016.

[3] M. Rinaldi, F. Parisi, G. Laskaris, A. D'Ariano, and F. Viti, in *2018 21st International Conference on Intelligent Transportation Systems (ITSC)*. IEEE, 2018, pp. 41–46.

[4] Y. Gao, S. Guo, J. Ren, Z. Zhao, A. Ehsan, and Y. Zheng, *Energies*, vol. 11, no. 8, p. 2060, 2018.

[5] A. Jahic, M. Eskander, and D. Schulz, *Applied Sciences*, vol. 9, no. 9, p. 1748, 2019.

[6] R. Guyot, B. Lasserre, J. Vicente, L. Torcheux, and L. Martin, in *Proceedings of the Electric Vehicle Symposium EVS-32, Lyon, France*, 2019, pp. 19–22.

[7] M. Jiang, Y. Zhang, C. Zhang, K. Zhang, G. Zhang, and Z. Zhao, in *2018 21st International Conference on Intelligent Transportation Systems (ITSC)*. IEEE, 2018, pp. 1894–1899.

[8] R.-C. Leou and J.-J. Hung, *Energies*, vol. 10, no. 4, p. 483, 2017.

[9] H. Chen, Z. Hu, Z. Xu, J. Li, H. Zhang, X. Xia, K. Ning, and M. Peng, in *2016 IEEE PES Asia-Pacific Power and Energy Engineering Conference (APPEEC)*. IEEE, 2016, pp. 1174–1179.

[10] G. Wang, X. Xie, F. Zhang, Y. Liu, and D. Zhang, in *2018 IEEE Real-Time Systems Symposium (RTSS)*. IEEE, 2018, pp. 45–55.

[11] T. Zhu, H. Min, Y. Yu, Z. Zhao, T. Xu, Y. Chen, X. Li, and C. Zhang, *Energies*, vol. 10, no. 2, p. 243, 2017.

[12] A. Houbbadi, E. Redondo-Iglesias, R. Trigui, S. Pelissier, and T. Bouton, in *2019 IEEE Vehicle Power and Propulsion Conference (VPPC)*. IEEE, 2019, pp. 1–6.

[13] R. Trigui, B. Jeanneret, and F. Badin, *RTS-Recherche Transports Securite*, no. 83, pp. 129–150, 2004.

[14] A. Houbbadi, R. Trigui, S. Pelissier, E. Redondo-Iglesias, and T. Bouton, *Energies*, vol. 12, no. 14, p. 2727, 2019.

[15] A. Genovese, F. Ortenzi, and C. Villante, *World Electric Vehicle Journal*, vol. 7, no. 4, pp. 570–576, 2015.

[16] A. Eddahech, O. Briat, E. Woirgard, and J.-M. Vinassa, *Microelectronics Reliability*, vol. 52, no. 9-10, pp. 2438–2442, 2012.

[17] S. Grolleau, A. Delaille, H. Gualous, P. Gyan, R. Revel, J. Bernard, E. Redondo-Iglesias, J. Peter, and S. Network, *Journal of Power Sources*, vol. 255, pp. 450–458, 2014.

[18] S. Grolleau, A. Delaille, and H. Gualous, in *2013 World Electric Vehicle Symposium and Exhibition (EVS27)*, 2013.

[19] E. Redondo-Iglesias, P. Venet, and S. Pelissier, *Journal of Energy Storage*, vol. 13, pp. 176–183, 2017.

[20] T. Waldmann, M. Wilka, M. Kasper, M. Fleischhammer, and M. Wohlfahrt-Mehrens, *Journal of Power Sources*, vol. 262, pp. 129–135, 2014.

[21] Z. Song, H. Hofmann, J. Li, J. Hou, X. Zhang, and M. Ouyang, *Applied energy*, vol. 159, pp. 576–588, 2015.

[22] M. Broussely, S. Herreyre, P. Biensan, P. Kasztejna, K. Nechev, and R. Staniewicz, *J. Power Sources*, vol. 97–98, pp. 13 – 21, 2001, proceedings of the 10th International Meeting on Lithium Batteries. [Online]. Available: http://www.sciencedirect.com/science/article/pii/S0378775301007224

[23] A. Houbbadi, R. Trigui, S. Pelissier, E. Redondo-Iglesias, and T. Bouton, *International Journal of Electric and Hybrid Vehicles*, vol. 11, 2019.